

Implications on accretion flow dynamics from spectral study of Swift J1357.2-0933

Santanu Mondal^{★1,2} and Sandip K. Chakrabarti^{†2,3}

¹*Instituto de Física y Astronomía, Facultad de Ciencias, Universidad de Valparaíso, Gran Bretana N 1111, Playa Ancha, Valparaíso, Chile*

²*Indian Centre for Space Physics, Chalanika 43, Garia Station Rd., Kolkata, 700084, India*

³*S. N. Bose National Centre for Basic Sciences, Kolkata, 700098, India*

ABSTRACT

We report a detailed spectral study of Swift J1357.2-0933 low-mass X-ray binary during its 2017 outburst using *Swift* and *NuSTAR* observations. We fit the data with two component advective flow (TCAF) model and power-law model. We observe that the source is in hard state during the outburst, where the size of the Compton cloud changes significantly with disc accretion rate. The typical disc accretion rate for this source is $\sim 1.5 - 2.0$ % of the Eddington accretion rate (\dot{M}_{Edd}). The model fitted intermediate shock compression ratio gives an indication of the presence of jet, which is reported in the literature in different energy bands. We also split *NuSTAR* data into three equal segments and fit with the model. We check spectral stability using color-color diagram and accretion rate ratio (ARR) vs. intensity diagram using different segments of the light curve but do not find any significant variation in the hardness ratio or in the accretion rate ratio. To estimate the mass of the candidate, we use an important characteristics of TCAF that the the model normalization always remains a constant. We found that the mass comes out to be in the range of $4.0 - 6.8 M_{\odot}$. From the model fitted results, we study the disc geometry and different physical parameters of the flow in each observation. The count rate of the source appears to decay in a time scale of ~ 45 day.

Key words: black hole physics, accretion, accretion discs, binaries: close, stars: individual (Swift J1357.2-0933)

1 INTRODUCTION

In a black hole binary, matter falls onto the compact object while transporting angular momentum outwards and mass inwards converting half of its gravitational potential energy into thermal energy and radiation energy. Thus, it is interesting to study the accretion dynamics both in temporal and spatial domains. Unlike a persistent source, where accretion rates could be steady for a long time, in an outburst source, rates are supposed to be varying. Outbursting black hole candidates (BHCs) spend most of the times in the quiescence state and occasionally undergo bright X-ray outbursts, which are definitely due to a huge increase of accretion rate. One of the most natural ways to achieve this is by varying viscosity. It is possible that an outburst may be triggered by enhancement of viscosity at the piling radius of matter. Chakrabarti (1990, 1996) suggested that when the rise of viscous process increases the viscosity parameter above a critical value, the low angular momentum flow can acquire a Keplerian distribution which becomes a SS73-like standard disk in presence of cooling (Shakura & Sunyaev, 1973). Based on this Chakrabarti (1997) concluded that the regular rise and fall of the

accretion rate is due to the enhancement and reduction of viscosity at the outer regions of the disc.

Transient BHCs show several components in their spectra, namely, blackbody, power-law and an iron line at around 6.4 keV. These distinct components are primarily from the optically thick and thin flow components. It is observed that the spectra change their shape during the outburst following a cycle from hard to soft through intermediate states i.e., see, the hardness intensity diagram (HID, Homan & Belloni 2005; Nandi et al. 2012). Several attempts were made to explain changes in the spectral shape and its variation (Remillard & McClintock 2006 for a review). However, there was a lack of physical understanding behind this. Most of the studies are qualitative and phenomenological. It is believed that changes in the accretion rate may be responsible for changes in spectral states (Maccarone & Coppi 2003; Meyer-Hofmeister et al. 2004 and references therein). However, causes of the change in accretion rate on a daily basis, the origin of corona and its temperature, optical depth etc. were not very clear.

The problems were satisfactorily resolved when proper usage of the solution of transonic flows in presence of viscosity was used. In a Two Component Advective Flow (TCAF, Chakrabarti & Titarchuk 1995, hereafter, CT95) solution, a Keplerian disc which arises out of higher viscosity is immersed inside a hot sub-Keplerian flow of lower viscosity. This sub-Keplerian, low angu-

[★] santanu.mondal@uv.cl

[†] chakraba@bose.res.in

lar momentum hot matter forms an axisymmetric shock due to the dominance of the centrifugal force (Chakrabarti 1990; Molteni, Lanzafame & Chakrabarti 1994). The subsonic region between the shock boundary to the inner sonic point is hot and puffed up and behaves as the Compton cloud, which upscatters intercepted soft photons from the standard disc. This region also supplies matter to the jet and outflow (Chakrabarti 1999a, hereafter C99a). This is called the CENTrifugal barrier dominated BOUNDary Layer or CENBOL. This region could be oscillatory when its cooling time scale roughly matches with the infall (compression) timescale inside CENBOL (MSC96; Chakrabarti & Manickam 2000; Chakrabarti et al. 2015). Recently, Chakrabarti et al. (2015) applied the resonance condition for H 1743-322 black hole candidate and showed that the low frequency quasi-periodic oscillations (LFQPOs) are produced when cooling time scale roughly matches with the infall time scale. Transonic solution by Mondal & Chakrabarti (2013; CT95) shows that cooling mechanism is also responsible for the change in spectral states. The presence of two components as in CT95 is established by many other authors in the literature (Smith et al. 2001, 2002; Wu et al. 2002; Ghosh & Chakrabarti, 2018).

After the implementation of TCAF in XSPEC (Debnath et al. 2014) and fitting data of several black hole candidates, one obtains physical parameters of the underlying inflow, such as the accretion rates of the disk and halo components, the shock location and the shock strength. If the mass is unknown, this will also be found out from the spectral fit (e.g., Molla et al. 2016; Bhatterjee et al. 2017). A plot of photon count variation with accretion rate ratio (ARR) gives the so call ARR intensity diagram (ARRID, Mondal et al. 2014b; Jana et al. 2016) and directly shows why the spectral state changes. The changes in accretion rates on a daily basis is due to changes in viscosity parameter during the outburst (Mondal et al. 2017). The time scale of the changes can also be estimated from the model fitted accretion rates (Jana et al. 2016). From the spectral fits, QPO frequencies can be predicted as well (Debnath et al. 2014; Chakrabarti et al. 2015; Chatterjee et al. 2016).

Till date, many faint X-ray binaries have been discovered and with even fainter companions. Swift J1357.2-0933 has one of the shortest orbital periods and is a very faint black hole X-ray transient. The source was first detected in 2011 by the *Swift* Burst Alert Telescope (Barthelmy et al. 2005; Krimm et al. 2011). The distance to the source is not confirmed. This can range from $\sim 1.5 - 6.3$ kpc (Rau et al. 2011; Shahbaz et al. 2013). There is also a large discrepancy in mass measurement of the source. The mass of the black hole is estimated to be $> 3.6 M_{\odot}$ by Corral-Santana et al. (2013) and $> 9.3 M_{\odot}$ by Mata Sánchez et al. (2015). Corral-Santana et al. (2013) also estimated the orbital period to be 2.8 ± 0.3 hrs from the time-resolved optical spectroscopy. They observed recurring dips on 2-8 min time-scales in the optical lightcurve, although the RXTE and XMM-Newton data do not show any of the above evidences (Armas Padilla et al. 2014). The observed broad, double-peaked H_{α} profile supports a high orbital inclination (Torres et al. 2015). Very recently, Russell et al. (2018) found an evolving jet synchrotron emission using long term optical monitoring of the source.

In the earlier outburst during 2011, the source had a variable accretion and showed very regular temporal and spectral evolution. The detailed multiwavelength lightcurve is studied by Weng & Zhang (2015). Recently, Swift J1357.2-0933 showed renewed activity on 2017 April 20 (Drake et al. 2017) and April 21 (Sivakoff et al. 2017, observed by Swift/XRT). Very recently, Stiele & Kong (2018) observed the source by NuSTAR and there is a simultaneous observation in Swift/XRT as well. Thus the present outburst covers

a broadband energy range. In this paper, we use the above data to study the flow dynamics of the source during its 2017 outburst.

The paper is organized as follows: in the next Section, we present the observation and data analysis procedure. In §3, we discuss about the model fitted results and geometry of the disc during the outburst. We also estimate the mass from the model fit. In §4, we calculate various physical quantities of the disc from model fitted parameters to infer about the disc properties. Finally, in §5, we draw our brief concluding remarks.

2 OBSERVATION AND DATA ANALYSIS

In the present manuscript, we analyze both Swift/XRT (Gehrel et al., 2004) and NuSTAR (Harrison et al. 2013) satellite observations of the BHC Swift J1357.2-0933 during its 2017 outburst.

2.1 Swift

In our present analysis, we use 0.5-7.0 keV Swift/XRT observation of Swift J1357.2-0933 during 2017 outburst, the timings of which overlap with the NuSTAR observations presented below. The observation IDs are 00088094002 (Photon Counting mode, PC) and 00031918066 (Windowed Timing mode, WT). We use *xrtpipeline* v0.13.2 task to extract the event fits file from the raw XRT data. All filtering tasks are done by *FTOOLS*. To generate source and background spectra we run *xselect* task. We use *swxpc0to4s6_20130101v014.rmf* and *swxwt0to2s6_20130101v015.rmf* file for the response matrix. The *grppha* task is used to group the data. We use 10 bins in each group. We use same binning for both the observations and also in NuSTAR data, which we discuss in the next section.

2.2 NuSTAR

We analyze two NuSTAR observations with observation IDs: 90201057002 (hereafter O1, combined with 00088094002) and 90301005002 (hereafter O2, combined with 00031918066) of BHC Swift J1357.2-0933 with energy range 2.0-70 keV. NuSTAR data were extracted using the standard NUSTARDAS v1.3.1 software. We run ‘nupipeline’ task to produce cleaned event lists and ‘nuproducts’ for spectral file generation. We use 30'' radius region for the source extraction and 45'' for the background using ‘ds9’. The data is grouped by ‘grppha’ command, where we group the whole energy bin with 10 bins in each group. We choose the same binning and fitting criteria for both the observations. However, the data quality of O2 is not good and above ~ 20 keV it is highly noisy. Thus the count at different energy ranges in O2 is not similar to O1. We split the NuSTAR observations into three different time ranges (S1, S2, and S3) each of which contains ~ 24 ksec (for O1) and ~ 15 ksec (for O2) data. For that purpose, first we make our own ‘GTI’ files for each time range using ‘gtibuild’ task in SAS environment and use those GTI files during data extraction. For spectral fitting of the data we use XSPEC (Arnaud, 1996) version 12.8.1. We fit the data using 1) Power-law (PL), and 2) TCAF models. The detailed spectral fitting with other phenomenological models and with reflection model (relxill) are discussed in Stiele & Kong (2018). Using relxill model and assuming high inclination, they found that the disc is truncated close to the black hole independent of spin parameter. Here, we mainly focus on the TCAF model fitted parameters to study the physical properties of the disc and its geometry during the outburst. To fit the spectra with the

TCAF model in XSPEC, we have a TCAF model generated *fits* file (Debnath et al. 2014). We follow the same analysis procedure for TCAF fitting with Swift and NuSTAR data as discussed in Mondal et al. (2016). We use the absorption model *TBabs* (Wilms et al. 2000) with hydrogen column density fixed at 1.3×10^{21} atoms cm^{-2} throughout the analysis. In the above absorption model solar abundance vector set to “wilm”, which includes cosmic absorption with grains and H_2 and those absorptions which are not included in the paper are set to zero. We keep the mass as a free parameter in order to estimate it from the TCAF itself.

3 MODEL FITTED RESULTS AND DISC GEOMETRY

We study the BHC Swift J1357.2-0933 using Swift/XRT and NuSTAR observations with PL model. PL model fitted photon index is $\sim 1.7 - 1.8$. Thus the object is in a hard state. We also fit the data with the TCAF solution based fits file which uses five physical parameters: The parameters are as follows (i) Mass of the black hole, (ii) disc accretion rate, (iii) halo accretion rate, (iv) location of the shock, and (v) shock compression ratio. Parameters (ii) to (v) collectively give the electron density and temperature, photon spectrum and density, the fraction of photons intercepted by the CENBOL from the disk, as well as the reflection of hard photons from the CENBOL by the disc. All of these depend on the mass of the black hole. According to CT95, if one increases the halo rate keeping other parameters frozen, the model will produce a hard spectrum. Similarly, increasing the disc rate leaving other parameters frozen, will produce a soft spectrum. When the location of the shock is increased keeping other parameters fixed, spectrum will be harder. A similar effect is seen for compression ratio also (see also, Chakrabarti 1997). In general, in an outburst, all the parameters will change smoothly in a multidimensional space. The model fitted results for both the observations are given in Table 1. In Fig. 1(a-b), we present the TCAF model fitted spectra. The model fitted parameters show that the disc rate was higher on the second day. Opposite is true for the halo rate. In both the observations, the ratio of the halo rate and disc rate is larger than unity, i.e., the flow is dominated by the sub-Keplerian rate. This is an indication of the hard state. At some point in time, before the second observation day, viscosity may have started to go up, and the Keplerian disc rate also started to increase. However, this was not enough so as to change the spectral state (as a minimum viscosity is required for such changes (Mondal et al. 2017)). The PL model fitted photon index also indicates a hard spectral state.

As the shock is the outer boundary of the Compton cloud, the movement of the shock shows a change in size of the Compton cloud. On the second day of observation, the shock moved closer to the black hole as compared to the first day from $X_s = 81.00 r_g$ to $\sim 36.66 r_g$ (where, Schwarzschild radius $r_g = 2GM_{BH}/c^2$). This type of behavior is observed routinely in all the black holes during the rising phase of the outburst. The behavior of advancing inner edge of the disc was studied by several authors for various outbursting candidates (Esin et al. 1997; Tomsick et al. 2009; Dutta & Chakrabarti 2010; Shidatsu et al. 2011; Nandi et al. 2012). The shock compression ratio (the ratio of the post-shock to pre-shock flow density experienced by the low angular momentum component) is always observed to be higher than unity and is generally of intermediate strength. In this case, the jets and outflows are expected to be strong (C99a; Chakrabarti 1999b). For the compression ratio given in the Table, the expected outflow/inflow ratio will be 3.4–4.2 %. This jet may appear and disappear during the transi-

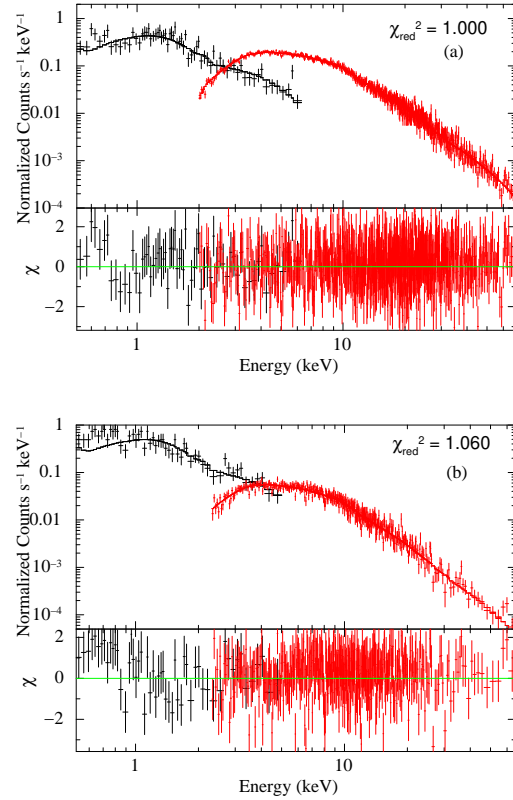


Figure 1. Swift/XRT and NuSTAR (focal plane module A, FPMA) data from 0.5-70.0 keV energy range are fitted with an absorbed TCAF model. The model fitted parameters are given in Table 1.

tion phase of the outburst, although the actual interrelation between the jet properties and the X-ray spectral state evolution is still debate (Kalemci et al. 2005; Dincer et al. 2014). Several attempts have been taken (Tomsick et al. 2009; Petrucci et al. 2014 and references therein) to understand the evolution of the Compton cloud and spectral state transitions as a function of luminosity during the outburst. Recent transonic solution of Mondal et al. (2014a) following the same flow geometry and jet configuration of C99a, showed that since the jet removes a significant amount of matter from CENBOL, it is easier to cool the Compton cloud. Thus, a change in spectral states in presence of jet is expected to be faster. Following the above model understanding and the values of the model fitted parameters, we conclude that the source was in rising hard state of the outburst during the observations.

In Fig. 2, we show the hardness intensity diagram (HID) and accretion rate ratio intensity diagram (ARRID) after splitting the data in three segments of equal time interval. The HID shows that the hardness ratio varied from 1.7 to 2.2. Thus one can say that the source is moderately variable. After fitting the data segments with TCAF model, we see that the ARR in ARRID varies by a factor of about 2. From both the diagrams, we note that the flow was not rapidly evolving.

In a series of papers with TCAF model fits, constant normalization was used for a given object observed by a given instrument as it is a conversion factor between the observed flux and the model flux. In Fig. 1, to fit the data we obtained model normalization 1.12 for NuSTAR observations, whereas Swift observations the fitting procedure produces the normalization values of 0.31 for O1 and

Table 1. PL and TCAF model fitted parameters of combined Swift/XRT and NuSTAR observation

Obs.	model1 (PL)	model2 (TCAF)
1	$\Gamma = 1.678 \pm 0.007$ $norm = 0.018 \pm 0.001$ $\chi^2/dof = 792.95/798$ — — —	$M_{BH} = 6.84 \pm 0.39$ $\dot{m}_d = 0.017 \pm 0.001$ $\dot{m}_h = 0.378 \pm 0.021$ $X_s = 81.04 \pm 7.91$ $R = 2.74 \pm 0.34$ $\chi^2/dof = 804.56/805$
2	$\Gamma = 1.811 \pm 0.015$ $norm = 0.0088 \pm 0.0003$ $\chi^2/dof = 451.98/442$ — — —	$M_{BH} = 4.01 \pm 0.34$ $\dot{m}_d = 0.019 \pm 0.004$ $\dot{m}_h = 0.213 \pm 0.013$ $X_s = 36.66 \pm 4.42$ $R = 2.0 \pm 0.16$ $\chi^2/dof = 473.12/446$

M_{BH} is in unit of M_\odot and Mass accretion rates are in \dot{M}_{Edd} unit.
 X_s is in $2GM_{BH}/c^2$ unit.

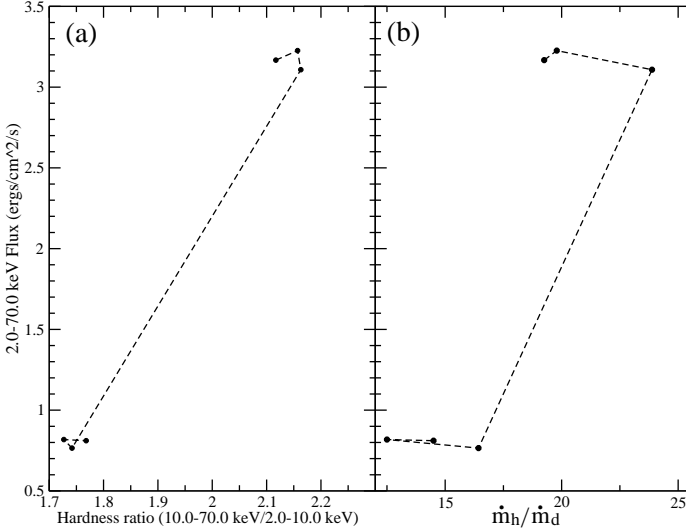


Figure 2. (a) Hardness ratio (10.0-70.0 keV/2.0-10.0 keV) of NuSTAR data for both the observations after splitting the data in three intervals mentioned in Sec. 2. Total flux is in $1.0E-10 \text{ ergs/cm}^2/\text{s}$ unit. (b) Variation of total flux with ARR. It is to be noted that the hardness ratio varies moderately between 1.7-2.2 and ARR by a factor of 2.

1.13 for O2. The freedom in absorption does not improve the fit significantly, rather gives a factor of 10 difference in N_H between O1 and O2. As the normalization is not chosen by hand and it comes out as a fitted parameter, the ratio of the normalizations is important. The relative normalization for the two instruments can be calculated from the ratio of the model normalizations obtained from the fits of each instrument's spectrum. There could be several reasons for getting different normalizations in Swift data in O1 and O2: 1) if the Swift and NuSTAR data are not strictly simultaneous, 2) there could be a pile-up issue, and 3) if the source is close to the PC/WT switch point, then it may be relatively faint for WT. As the source was not highly variable during that period, the point 1 cannot be a reason for the difference in normalization. The pile-up could be an issue as the count rate is above 0.5 cnts/sec. We should mention that we have performed the analysis using pile-up corrected spectrum files for PC mode generated by online Swift/XRT product generator (Evans et al. 2009). However, the difference in normalization persists. The model fitted parameter values also remained

unchanged with an acceptable reduced χ^2 (~ 1.0) keeping the mass of the source within $4.0 M_\odot - 6.8 M_\odot$. The third point should not be the reason for difference in normalization as the source is sufficiently bright for WT mode.

These leads us to conclude that the difference in normalization could be due to other physical processes inside the accretion disc which were not incorporated in TCAF. As discussed in Jana et al. (2016) and Molla et al. (2017), the presence of jet is a reason for the difference in normalization. During the present outburst period, activity in jet was observed for this source. Thus the presence of jet/outflow could be a reason behind the variation of normalization constant.

4 ESTIMATION OF DIFFERENT PHYSICAL QUANTITIES OF THE DISC

In this Section, we estimate some physical parameters of the disc using TCAF model fitted parameters. From Kepler's law, one can derive a relation between orbital period (P) and orbital separation a as follows:

$$a = 3.5 \times 10^{10} m_2^{1/3} (1 + q)^{1/3} P(\text{hr})^{2/3}, \quad (1)$$

where $q (= m_1/m_2)$ is the mass ratio of the component stars. Outer disc radius (r_{out}) of the primary star is calculated from the Roche lobe radius of the primary following Eggleton (1983) as,

$$r_{Rl,1} = \frac{0.49 \times a q^{2/3}}{0.6 \times q^{2/3} + \ln[1 + q^{1/3}]}. \quad (2)$$

In this work, we consider that the outer edge of the disc (r_{out}) is 70% of the Roche lobe radius. We use the values of P ($= 2.8 \text{ hrs}$) and companion mass ($= 0.17 M_\odot$) in Eq. 2, already derived by Corral-Santana et al. (2013), to estimate Roche lobe radius, which appears to be $r_{out} = 0.68 \times 10^{11}$. Using the above derived outer disc radius and model fitted accretion rate, we calculate kinematic viscosity (ν) and surface density (Σ) of the disc. It is to be noted that the disc accretion rate which we are using from TCAF fit is constant throughout the disc, thus we assume that the accretion at r_{out} is same as the model fit value. We use standard disc equations (SS73) below to derive the above two physical parameters (ν and Σ):

$$\Sigma \simeq \frac{\dot{M}_d}{3\pi\nu}, \quad (3)$$

where, ν is calculated using SS73 α disc model ($\nu = \alpha C_s H$). Here $C_s^2 (= \frac{kT}{\mu m_p})$ and $H (= \frac{C_s}{\Omega_K} = 0.024)$ are the sound speed at the outer radius of the disc, height of the disc and Ω_K is the Keplerian angular velocity at that point respectively. The temperature of the disc is calculated from the disc accretion rate. The estimated values of Σ and ν are $\sim 49.1 \text{ gm/cm}^2$ and $\sim 4.0 \times 10^{14} \text{ cm}^2/\text{sec}$ respectively. During our calculation, we consider that the disc is not self-gravitating i.e., vertical hydrostatic equilibrium is maintained against the pull of the gravity. The computed low surface density and kinematic viscosity are indicating a stable disc. In the context of disc stability, Weng & Zhang (2015) mentioned that the high ratio of near UV luminosity to X-ray luminosity indicates that the irradiation is unimportant in this outburst, while the near-exponential decay profile and the long decay time-scale conflicts with the disc thermal-viscous instability model. Hence they suggested that the disc is thermally stable during the outburst. Armas Padilla et al. (2013) also found that the correlation between Swift/UVOT v-band and XRT data is consistent with a non-irradiated accretion disc.

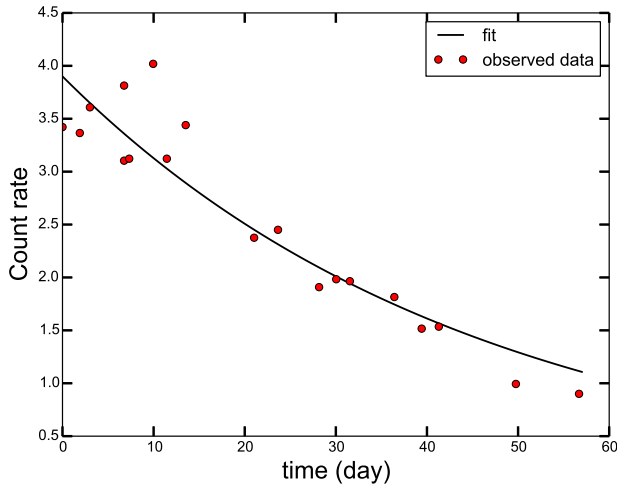


Figure 3. Variation of count rate with time (day). Black solid line shows the model fit and filled circles are observed count rates. Data are fitted with $H/R = 0.024$ (from above), $P = 2.8$ hrs, $q = 0.03$ and SS73 $\alpha = 0.25$. Count rate of Swift lightcurve is adopted from Stiele & Kong (2018).

Here, we present the chain of logical steps used to fit the observed lightcurve: (i) we have mass and disc accretion rate from TCAF fit, (ii) using (i) we estimate disc temperature thus the sound speed, (iii) we also have orbital period (P) and mass function (q) from literature, (iv) outer disc radius is estimated using Eq. 1 from the parameters of (iii), (v) once (ii) and (iv) are known one can estimate height of the disc, Keplerian angular frequency, and disc kinematic viscosity to estimate the viscous time scale, and (vi) finally, we extract SS73- α parameter for which the derived and the fitted τ values are consistent. Here, α takes the value 0.25 to give a decay timescale (τ) of ~ 45 days. To fit the observed count rate using decay timescale, we use an exponential decay function, which is given by:

$$f = A \exp(-t/\tau), \quad (4)$$

where A is a normalization constant, which takes the value of 3.91 ± 0.16 with exponential decay timescale (τ) around 45.28 ± 4.78 days. The estimated SS73 disc viscosity parameter ($\alpha = 0.25$) becomes same order as those obtained for other observed candidates (Nagarkoti & Chakrabarti 2016; Mondal et al. 2017). Here we consider A as a constant, however it should depend on the source distance and the physical properties of the disc. The detailed calculation is beyond the scope of this paper. In Fig. 3, we show exponential decay function fitted with the observed count rate.

5 SUMMARY AND CONCLUSIONS

In this paper, we analyzed Swift/XRT and NuSTAR spectra of a known Galactic stellar mass black hole source Swift J1357.2-0933 during its 2017 outburst using a phenomenological PL model and a physical TCAF solution. We find that on both the observation dates, the sub-Keplerian halo accretion rate is higher than the Keplerian accretion rate. In the second observed day, the disc rate is increased as compared to first observed day and opposite variation is seen in the sub-Keplerian rate. The object was in hard state on both the days. As the halo rate is higher than the disc rate and the shock

compression ratio is always greater than unity, the shock moved inward due to cooling. This could be the signature of the hard state in the rising phase of the outburst. The shock was seen to move at ~ 0.15 m/s which is similar to the shock velocity in other outbursts (Debnath et al. 2010 for GX 339-4; Mondal et al. 2015 for H 1743-322 and references therein). This indicates that the outburst probably remained in the rising phase and no other spectral state has been missed in between these ~ 40 days. It is to be noted that the companion of this candidate is a star evolved through nuclear fusion (Shahbaz et al. 2013) with an initial mass $\sim 1.5 M_{\odot}$, which has evolved to $0.17 M_{\odot}$. Thus there is a possibility that the accretion is mostly dominated by companion winds and thus the halo rate is always higher. Our model fitted disc rate is $\sim 1.5 - 2\%$ of \dot{M}_{Edd} . As the disc rate increases and the shock location decreased in ~ 40 days, viscosity must have gone up since the first observation. As the shock compression ratio is in intermediate strength, in this case, the jets and outflows are expected to be strong with outflow/inflow rate ratio 3.4-4.2%. From TCAF model fit, we estimate the mass range for this black hole candidate to be $4.0 - 6.8 M_{\odot}$. However, a few more observations would have reduced the error-bar significantly.

We also study different physical parameters of the disc. For that, we calculate the surface density, kinematic viscosity and disc aspect ratio etc. of the disc using the model fitted parameters. We find that the disc surface density is not high enough signifying that the disc is stable in nature. The estimated surface density is also reasonable to produce a consistent α value to study the decay of the lightcurve. We find that the lightcurve fits with exponential decay function with the decay time scale of ~ 45 day, which is consistent with the derived decay time scale when $\alpha=0.25$. Thus from the model fit we can study the spectra, disc properties, lightcurve decay and estimate viscosity parameter at a time.

6 ACKNOWLEDGMENT

We thank anonymous referee for useful comments on the manuscript. SM acknowledges Swift team (especially Kim Page) for useful discussions on Swift data fitting and Patricia Arévalo for commenting on the preliminary version of the paper. SM acknowledges FONDECYT fellowship grand (# 3160350) for this work. This research has made use of the NuSTAR Data Analysis Software (NuSTARDAS) jointly developed by the ASI Science Data Center (ASDC, Italy) and the California Institute of Technology (Caltech, USA), and the XRT Data Analysis Software (XRTDAS) developed under the responsibility of the ASI Science Data Center (ASDC), Italy. This research has made use of data obtained through the High Energy Astrophysics Science Archive Research Center Online Service, provided by the NASA/Goddard Space Flight Center.

REFERENCES

- Armas Padilla, M., Degenaar, N., Russell, D. M., & Wijnands, R. 2013, MNRAS, 428, 3083
- Armas Padilla, M., Wijnands, R., Altamirano, D., et al. 2014, MNRAS, 439, 3908
- Arnaud, K.A., ASP Conf. Ser., Astronomical Data Analysis Software and Systems V, ed. G.H. Jacoby & J. Barnes, 101, 17 (1996)
- Bhattacharjee, A., Banerjee, I., Banerjee, A., et al. 2017, MNRAS, 466, 1372
- Chakrabarti, S. K. 1989, MNRAS, 240, 7

- Chakrabarti, S. K. 1990, *ApJ*, 362, 406
- Chakrabarti, S. K. 1996, *ApJ*, 464, 664
- Chakrabarti, S. K. 1997, *ApJ*, 484, 313
- Chakrabarti, S. K. 1999a, *A & A*, 351, 185
- Chakrabarti, S. K. 1999b, *Ind. J. Phys.*, 73B, 6, 931
- Chakrabarti, S. K., & Titarchuk, L.G. 1995, *ApJ*, 455, 623
- Chakrabarti, S. K., & Manickam, S. G. 2000, *ApJ*, 531, L41
- Chakrabarti, S. K., Mondal, S. & Debnath, D. 2015, *MNRAS*, 452, 3451
- Chatterjee, D., Debnath, D., Chakrabarti, S. K., et al. 2016, *ApJ*, 827, 88
- Corral-Santana, J. M., Casares, J., & Muñoz-Darias, T., et al. 2013, *Science*, 339, 1048
- Debnath, D., Chakrabarti, S. K., & Mondal, S. 2014, *MNRAS*, 440, L121
- Debnath, D., Mondal, S., & Chakrabarti, S. K. 2015, *MNRAS*, 447, 1984
- Debnath, D., Chakrabarti, S. K., & Nandi, A. 2010, *A&A*, 520, 98
- Dincer, T., Kalemci, E., Tomsick, J. A., et al., 2014, *ApJ*, 795, 74
- Dutta, B. G., & Chakrabarti, S. K. 2010, *MNRAS*, 404, 2136
- Eggleton, P. P. 1983, *ApJ*, 268, 368
- Esin, A. A., McClintock, J. E., & Narayan, R. 1997, *ApJ*, 489, 865
- Evans, P. A., Beardmore, A. P., Page, K. L. 2009, *MNRAS*, 397, 1177
- Gehrels et al., 2004, *ApJ*, 611, 1005
- Ghosh, A. & Chakrabarti, S.K., 2018, *MNRAS*, 479, 1210
- Harrison, F. A., Craig, W. W., & Christensen, F. E., et al., 2013, *ApJ*, 770, 103
- Homan J., & Belloni T. 2005, *Ap&SS*, 300, 107
- Jana, A., Debnath, D., Chakrabarti, S. K., et al. 2016, *ApJ*, 819, 107
- Kalemci, E., Tomsick, J. A., Buxton, M. M., et al., 2005, *ApJ*, 622, 508
- Krimm, H. A., Barthelmy, S. D., Baumgartner, W., et al. 2011, *The Astronomers Telegram*, 3138
- Maccarone, T. C., & Coppi, P. S. 2003, *MNRAS*, 338, 189
- Mata Sánchez, D., Muñoz-Darias, T., Casares, J., Corral-Santana, J. M., & Shahbaz, T. 2015, *MNRAS*, 454, 2199
- McClintock, J. E. & Remillard, R. A. 2006, in *Compact Stellar X-ray Sources*, Cambridge, Astrophysical Ser., vol. 39, ed. W. Lewin & M. van der Klis (Cambridge Univ. Press), 157
- Meyer-Hofmeister, E., Liu, B. F., & Meyer, F. 2004, *A&A*, 432, 181
- Molla, A. A., Debnath, D., Chakrabarti, S. K., et al. 2016, *MNRAS*, 460, 3163
- Molla, A. A., Chakrabarti, S. K., Debnath, D., et al. 2017, *ApJ*, 834, 88
- Molteni, D., Lanzafame, G., & Chakrabarti, S. K. 1994, *ApJ*, 425, 161
- Molteni, D., Sponholz, H., & Chakrabarti, S. K. 1996, *ApJ*, 457, 805
- Mondal, S. & Chakrabarti, S. K. 2013, *MNRAS*, 431, 2716
- Mondal, S., Chakrabarti, S. K., & Debnath, D. 2014a, *Ap&SS*, 353, 223
- Mondal, S., Debnath, D., & Chakrabarti, S. K. 2014b, *ApJ*, 786, 4
- Mondal, S., Chakrabarti, S. K., & Debnath, D. 2015, *ApJ*, 798, 57
- Mondal, S., Chakrabarti, S. K., & Debnath, D. 2016, *Ap&SS*, 361, 309
- Mondal, S., Chakrabarti, S. K., Nagarkoti, S., & Arévalo, P. 2017, *ApJ*, 850, 47
- Nagarkoti, S., & Chakrabarti S. K. 2016, *MNRAS*, 462, 850
- Nandi A., Debnath D., Mandal S., & Chakrabarti S. K. 2012, *A&A*, 542, 56
- Petrucchi, P. O., Cabanac, C., Corbel, S., et al., 2014, *A&A*, 564, A37
- Rau, A., Greiner, J., & Filgas, R. 2011, *The Astronomers Telegram*, 3140
- Russell, D. M., Qasim, A. A., Bernardini, E., et al. 2018, *ApJ*, 852, 90
- Shakura, N. I., & Sunyaev, R. A. 1973, *A&A*, 24, 337
- Shahbaz, T., Russell, D. M., Zurita, C., et al. 2013, *MNRAS*, 434, 2696
- Shidatsu, M., et al., 2011, *PASJ*, 63, 785
- Sivakoff, G. R., Tetarenko, B. E., Shaw, A. W., & Bahramian, A. 2017, *The Astronomers Telegram*, No. 10314, 314
- Smith, D. M., Heindl, W. A., Markwardt, C. B., et al., 2001, *ApJL*, 554, L41
- Smith, D. M., Heindl, W. A., & Swank, J. H., 2002, *ApJ*, 569, 362
- Stiele, H., & Kong, A. K. H. 2018, *ApJ*, 852, 34
- Tomsick, J. A., Yamaoka, K., Corbel, S., et al. 2009, *ApJ*, 707, L87
- Torres, M. A. P., Jonker, P. G., Miller-Jones, J. C. A., et al. 2015, *MNRAS*, 450, 4292
- Weng, S.-S., & Zhang, S.-N., 2015, *MNRAS*, 447, 486
- Wilms, J., Allen, A., & McCray, R. 2000, *ApJ*, 542, 914
- Wu, K., Soria, R., Campbell-Wilson, D., et al., 2002, *ApJ*, 565, 1161